PROBLEMS OF MECHATRONICS
ARMAMENT, AVIATION, SAFETY ENGINEERING

ISSN 2081-5891

7, 1 (23), 2016, 7-16

Analysis of Aerodynamic Characteristics of the Rocket-Target for the „Stinger" System

Algimantas FEDARAVIČIUS*, Sigitas KILIKEVIČIUS, Arvydas SURVILA, Laima PATAŠIENĖ

Kaunas University of Technology, 27 Kęstučio Str., 44025 Kaunas, Lithuania
**corresponding author, e-mail: algimantas.fedaravicius@ktu.lt*

Manuscript received July 05, 2014. Final manuscript received March 21, 2015

DOI 10.5604/20815891.1195197

Abstract. This paper presents an analysis of aerodynamic characteristics of the rocket-target for the final training of shooting at aerial targets by the „Stinger" system service staff. The governing equations of fluid dynamics are presented and the computational model of airflow around the rocket is developed. ANSYS CFX computational fluid dynamics software is used to compute airflow velocities, pressure, the drag force and the drag coefficient. A practical implementation of the research is presented. Taking into account the simulation results, the rocket-target was designed and manufactured.
Keywords: aerodynamics, drag force, drag coefficient, rocket-target

1. INTRODUCTION

The geometrical and design parameters as well as the exterior ballistics characteristics of a rocket are usually estimated for a particular rocket design. The range of the rocket's velocities can be rather wide. The presented analysis was inspired by the demand to develop a rocket-target for the system „Stinger" which is about 5 meters in length and 0.4 meters in diameter.

This paper is based on the work presented at the 10th International Armament Conference on „Scientific Aspects of Armament and Safety Technology", Ryn, Poland, September 15-18, 2014.

The maximum speed of the rocket is intended to be less than 250 m/s. In this case one of optimal nose cones for the rocket is parabolic one [1, 2]. It is known that the airflow characteristics and its parameters such as airflow velocity, pressure, the drag force and etc. have a great influence on the exterior ballistics of the rocket. The drag force and the drag coefficient are the most important aerodynamic parameters necessary for the investigation of exterior ballistics, therefore, the necessary rocket engine thrust characteristics are directly related to these parameters.

Computational fluid dynamics (CFD) is now widely used in aeronautical applications to evaluate aerodynamic performance during the conceptual and preliminary design stages because of the demand to reduce the design cycle time and minimise the costs associated with experimental validation [3-5].

This paper deals with aerodynamic analysis of the rocket-target to be designed and the main objective is to obtain the drag force and the drag coefficient in the velocity range of 0.3-0.8 Mach number.

2. GOVERNING EQUATIONS

The airflow around the rocket was simulated using the commercial finite element software ANSYS CFX. The set of equations solved by ANSYS CFX are the unsteady Navier–Stokes equations in their conservation form [6].

The continuity equation:

$$\frac{\partial \rho}{\partial t} + \nabla \cdot (\rho U) = 0 \tag{1}$$

where ρ is the density and U is the vector of velocity.

The momentum equations:

$$\frac{\partial (\rho U)}{\partial t} + \nabla \cdot (\rho U \otimes U) = -\nabla p + \nabla \cdot \tau + S_M \tag{2}$$

where p is the pressure, S_M is the momentum source, τ is the stress tensor, which is related to the strain rate by:

$$\tau = \mu \left(\nabla U + (\nabla U)^T - \frac{2}{3} \delta \nabla \cdot U \right) \tag{3}$$

where δ is the Kronecker delta function (identity matrix) and μ is the molecular (dynamic) viscosity.

The total energy heat transfer model was used in this study which models the transport of enthalpy and includes kinetic energy effects.

The total energy equation:

$$\frac{\partial(\rho h_{tot})}{\partial t} - \frac{\partial p}{t} + \nabla \cdot (\rho U h_{tot}) = \nabla(\lambda \nabla T) + \nabla \cdot (U \cdot \tau) + U \cdot S_M + S_E \tag{4}$$

where h_{tot} is the total enthalpy, related to the static enthalpy $h(T, p)$ by:

$$h_{tot} = h + \frac{1}{2}U^2 \tag{5}$$

where λ is the thermal conductivity, T is the temperature and S_{E} is the energy source.

For turbulent flows, the instantaneous equations are averaged leading to additional terms. However, the averaging procedure introduces additional unknown terms containing products of the fluctuating quantities, which act like additional stresses in the fluid. These terms called Reynolds stresses need to be modelled by additional equations. These equations define the type of turbulence model [6].

In this study, the shear stress transport (SST) turbulence model was applied which is the most suitable for aeronautics flows with strong adverse pressure gradients and separation. The model (written in a conservation form) is given by the following [7]:

$$\frac{\partial(\rho k)}{\partial t} + \frac{\partial(\rho U_i k)}{\partial x_i} = \tilde{P}_k - \beta^* \rho k \omega + \frac{\partial}{\partial x_i}\left[(\mu + \sigma_k \mu_t)\frac{\partial k}{\partial x_i}\right] \tag{6}$$

$$\begin{aligned}\frac{\partial(\rho\omega)}{\partial t} + \frac{\partial(\rho U_i \omega)}{\partial x_i} &= \alpha\rho S^2 - \beta\rho\omega^2 + \frac{\partial}{\partial x_i}\left[(\mu + \sigma_\omega \mu_t)\frac{\partial \omega}{\partial x_i}\right] + \\ &+ 2(1 - F_1)\rho\sigma_{w2}\frac{1}{\omega}\frac{\partial k}{\partial x_i}\frac{\partial \omega}{\partial x_i}\end{aligned} \tag{7}$$

where k is the turbulence kinetic energy, ω is the turbulence frequency and μ_{t} is the turbulent viscosity. The blending function F_1 is defined by:

$$F_1 = \tanh\left\{\left\{\min\left[\max\left(\frac{\sqrt{k}}{\beta^*\omega y}, \frac{500v}{y^2\omega}\right), \frac{4\rho\sigma_{\omega 2}k}{CD_{k\omega}y^2}\right]\right\}^4\right\} \tag{8}$$

where y is the distance from the field point to the nearest wall.

$$CD_{k\omega} = \max\left(2\rho\sigma_{\omega 2}\frac{1}{\omega}\frac{\partial k}{\partial x_i}\frac{\partial \omega}{\partial x_i}, 10^{-10}\right) \tag{9}$$

F_1 is equal to zero away from the surface (k-ε model), and switches over to one inside the boundary layer (k-ω model).

The turbulent eddy viscosity is defined as follows:

$$v_t = \frac{a_1 k}{\max\left(a_1 \omega, SF_2\right)} \tag{10}$$

where $v_t = \mu_y/\rho$, S is the invariant measure of the strain rate and F_2 is the second blending function:

$$F_2 = \tanh\left\{\left[\max\left(\frac{2\sqrt{k}}{\beta^* \omega y}, \frac{500v}{y^2 \omega}\right)\right]^2\right\} \tag{11}$$

A production limiter is used in the SST model to prevent the build-up of turbulence in stagnation regions:

$$P_k = \mu_t \frac{\partial U_i}{\partial x_j}\left(\frac{\partial U_i}{\partial x_j} + \frac{\partial U_j}{\partial x_i}\right) \rightarrow \tilde{P}_k = \min\left(P_k, 10 \cdot \beta^* \rho k \omega\right) \tag{12}$$

The constants for the SST model are: $a_1 = 0.31$, $\beta^* = 0.09$, $\alpha_1 = 5/9$, $\beta_1 = 3/40$, $\sigma_{k1} = 0.85$, $\sigma_{\omega 1} = 0.5$, $\alpha_2 = 0.44$, $\beta_2 = 0.0828$, $\sigma_{k2} = 1$, $\sigma_{\omega 2} = 0.856$.

3. COMPUTATIONAL MODEL OF AIRFLOW AROUND THE ROCKET

The airflow around a rocket frame with nose and nozzle cones and around a rocket frame without a nozzle cone was investigated (Fig. 1). The diameter of the rockets is 0.4 m. The rocket „A" (Fig. 1a) does not have a nozzle cone at the end. The length of this rocket is 5 m. The length of the rocket with the nozzle cone is 5.2 m and the diameter of the nozzle cone end is 0.15 m. The length of the nose cone for the rocket „B" is 0.6 m (Fig. 1b) and the overall dimension between the fins is 1.6 m.

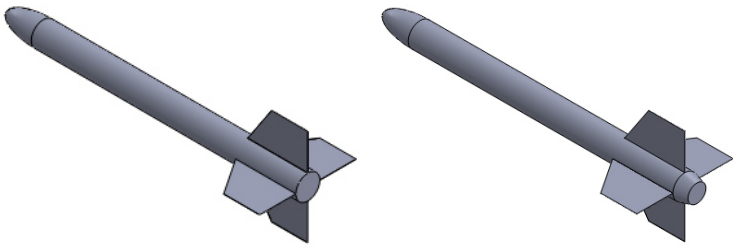

a b

Fig. 1. Investigated rockets: a – with the 0.6 m length nose cone and without a nozzle cone at the end; b – with the 0.6 m length nose cone

Computational numerical finite element models for a numerical simulation of airflow around the rockets were generated in ANSYS CFX software. Only a half of each model is discretized with a symmetry boundary condition. A rectangular fluid domain was placed around the rocket. The limit upstream of the body was located at a distance of 3 rocket's lengths and the limit downstream of the body was located at a distance of 5 rocket's lengths, whereas the lateral boundaries were placed at a distance of about 35 diameters (about 2.5 rocket's lengths). The mesh is of hybrid type, i.e. made up of prismatic elements in the viscous region located in close proximity of the body, whereas tetrahedral elements have been used to fill the remaining fluid volume. After a mesh sensitivity analysis, the maximum size of tetrahedral elements in the grid was set to 13.5 m and the minimum size was 7.5 mm. 20 inflation layers of prism elements were created on the surface of the rocket with the total thickness of 15 mm and the growth rate 1.2. On the surface of the rocket the mesh was made distinctly denser, the size of prism elements was set to 3.75 mm. The grid contains an overall size of about 7.18 million elements including about 3.5 million prism elements (Fig. 2).

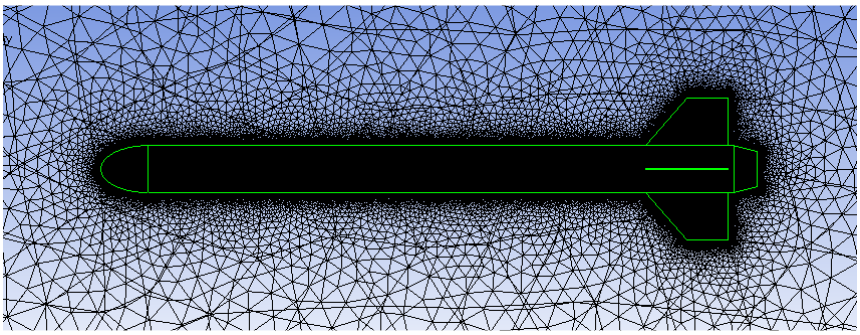

Fig. 2. CFD mesh

The maximum aspect ratio was 99 and occurred in the inflation layers, the maximum aspect ratio of the tetrahedron cells was 21.4 and the minimum aspect ratio was 1.15 while the average aspect ratio of all cells was 9.6. The maximum value of skewness was 0.88 while the average was 0.175, likewise the minimum orthogonal quality was 0.031 while the average was 0.907.

The Mach number of the flow at the inlet was changed from 0.3 to 0.8 during the simulation. At the outlet the relative static pressure was set to 0. Air temperature is 15°C and the reference pressure is 101325 Pa. The surface of the rocket was defined as a non-slippery smooth wall. The outside walls of the computational domain (the lateral boundaries) were defined as free slip walls.

The analysis was carried out taking into account heat exchange option and considering the compressible formulation of the Navier–Stokes equation system.

4. RESULTS OF THE AIRFLOW SIMULATION

The airflow velocity distribution on the cross-section plane, when the Mach number is 0.8, for the rocket „A" is showed in Fig. 3a and for the rocket „B" in Fig. 3b.

Velocity streamlines are showed in Fig. 4 (the local values of velocity are showed in the streamlines' legends).

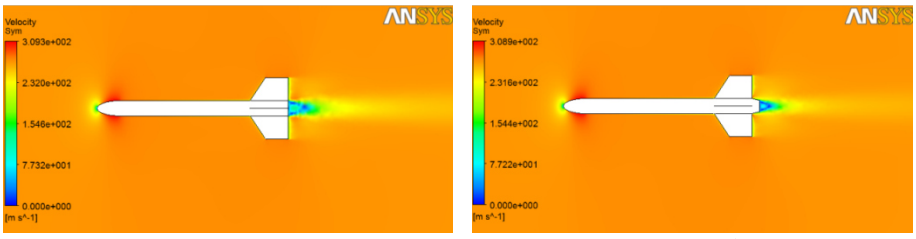

a b

Fig. 3. Velocity distribution on the cross-section plane under $M = 0.8$:
a – the rocket „A"; b – the rocket „B"

The pressure distribution on the frames of the rockets is shown in Fig. 5. Pressure distribution contours on the cross-section plane, when the Mach number is 0.8, for the rocket „A" are shown in Fig. 6a and for the rocket „B" are shown in Fig. 6b. The maximum value of pressure is a little bit higher for the rocket „A". The total pressure distribution on the cross-section plane under $M = 0.8$ is shown in Fig. 7.

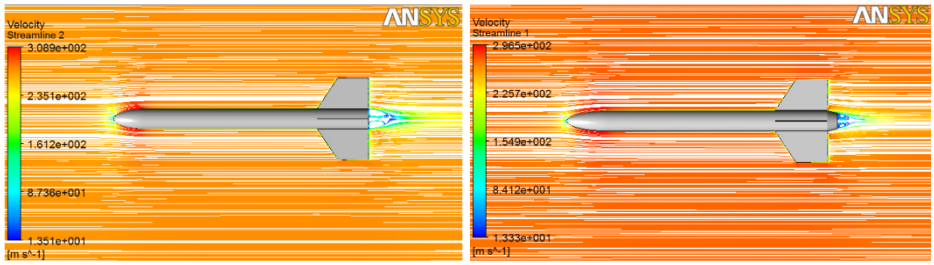

a b

Fig. 4. Velocity streamlines on the cross-section plane under $M = 0.8$:
a – the rocket „A"; b – the rocket „B"

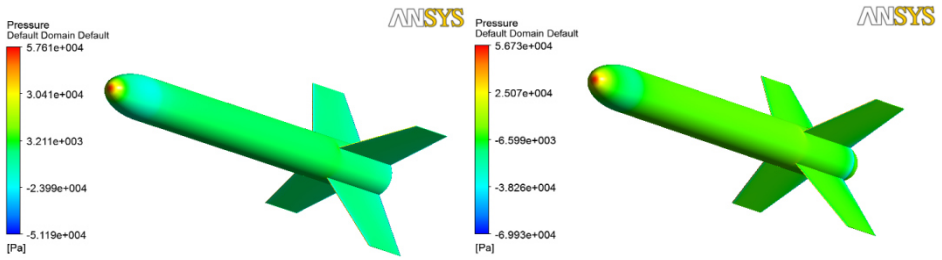

a b

Fig. 5. Pressure distribution on the rocket frame under M = 0.8:
a – the rocket „A"; b – the rocket „B"

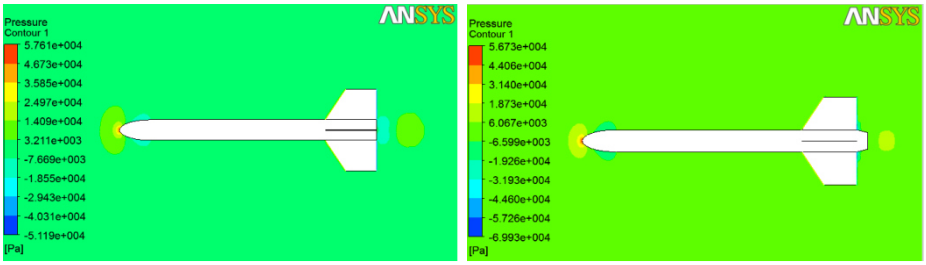

a b

Fig. 6. Pressure distribution under M = 0.8: a – the rocket „A"; b – the rocket „B"

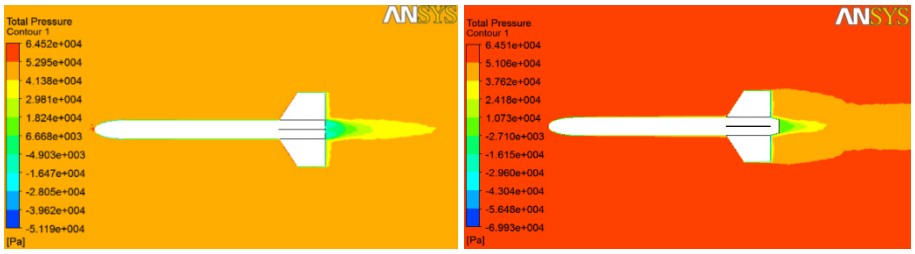

a b

Fig. 7. Total pressure distribution under M = 0.8: a – the rocket „A"; b – the rocket „B"

The drag coefficient was calculated by the following expression [8]:

$$C_d = \frac{F_d}{0.5\rho U^2 A} \tag{13}$$

where F_d is the drag force, obtained from the simulation results; ρ is the air density; U is the velocity of airflow; and A is the reference area.

The calculated drag force of the rocket „B" is significantly lower compared to the drag force of the rocket „A" (Fig. 8a). The drag force of the rocket „A" reaches up to 2753 N when M = 0.8, while the drag force of the rocket „B" reaches up to 19162 N. The drag coefficient of the rocket „B" is from 27% (at M = 0.3) to 29% (at M = 0.8) lower compared to the drag coefficient of the

rocket „A” (Fig. 8b). The calculated drag coefficient of the rocket „A” varies in the range of 0.42-0.44 depending on the velocity while the drag coefficient of the rocket „B” varies in the range of 0.29-0.32.

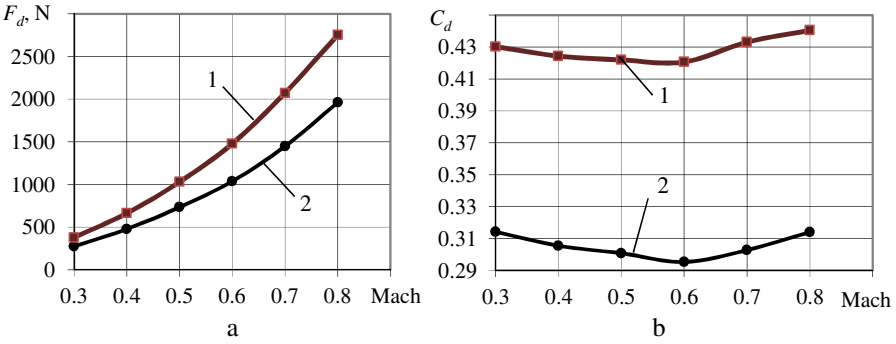

Fig. 8. Dependences of the drag force (a) and the drag coefficient (b) on the Mach number for: 1 – the rocket „A”; 2 – the rocket „B”

5. PRACTICAL IMPLEMENTATION

The purpose of the rocket-target is the final training of shooting at aerial targets by the „Stinger” system service staff. The rocket-target must satisfy all military training equipment requirements: it must be cheap, safe and it must fully meet the technical characteristics of the „Stinger” system. With that in mind and taking into account the simulation results, the rocket-target was designed and manufactured (Fig. 9). External ballistics calculations were performed using the obtained drag characteristics. The rocket-target „B” frame was accepted for the design and cheap composite materials were used for the rocket‘s body. Solid propellant for the rocket engine was used, which is distinguished by its ecological properties. The design of the rocket ensures visibility in the radio and infrared ranges. Technical characteristics of the rocket-target are presented in Table 1.

Table 1. Technical characteristics of the rocket-target

Technical characteristics	
Rocket length	5.4 m
Rocket diameter	0.4 m
Rocket mass	85-90 kg
Rocket velocity	160-250 m/s
Attitude of flight	up to 3.0 km
Flight distance	up to 8 km
Flight time	up to 45 s
Impulse	32 000 Ns
Burn time	3.5 s
Rocket complex mass (2 rockets)	950 kg

The rocket-target was successfully launched and served its purpose during military exercises (Fig. 8). The actual flight trajectory of the rocket-target was very close to the external ballistics calculations.

Fig. 9. Experimental example of the rocket-target complex

Fig. 10. Launching of the rocket during military exercises in the Baltic Sea

6. CONCLUSIONS

Computational airflow simulations around a rocket-target frame with nose and nozzle cones and around a rocket-target frame without a nozzle cone were performed and the necessary aerodynamics characteristics for computations of exterior ballistics were obtained.

The calculated drag force of the rocket with the nozzle cone is significantly lower compared to the drag force of the rocket without it. Accordingly, the drag coefficient of the rocket with the nozzle cone is from 27% (at M = 0.3) to 29% (at M = 0.8) lower compared to the drag coefficient of the rocket without it. The drag coefficient of the rocket with the nozzle cone varies in the range of 0.42-0.44 depending on the velocity while the drag coefficient of the rocket without it varies in the range of 0.29-0.32.

On the basis of the research results the rocket-target for the system „Stinger" was designed and manufactured. It was successfully launched and served its purpose during military exercises. The actual flight trajectory of the rocket-target was very close to the external ballistics calculations obtained using drag characteristics from the simulation results.

REFERENCES

[1] Department of Defense.1990. *Military Design Handbook. Design of Aerodynamically Stabilized Free Rockets*, U.S. Army Missile Command.

[2] Fedaravičius A., S. Kilikevičius, A. Survila. 2012. "Optimization of the rocket's nose and nozzle design parameters in respect to its aerodynamic characteristics". *Journal of Vibroengineering, Vilnius: Vibromechanika* 14(3) : 1390-1398.

[3] Langtry R.B., M. Kuntz, F. Menter. 2005. "Drag prediction of engine-airframe interference effects with CFX-5". *Journal of Aircraft*, 42(6) : 1523-1529.

[4] Kroll N., C.C. Rossow, D. Schwamborn, K. Becker, G. Heller. 2002. MEGAFLOW-a numerical flow simulation tool for transport aircraft design. In *Proceedings of ICAS Congress*, 1105.1-1105.20.

[5] Schütte A., G. Einarsson, A. Madrane, B. Schöning, W. Mönnich, W.R. Krüger. 2002. Numerical simulation of maneuvering aircraft by CFD and flight mechanic coupling, *RTO Symposium*. Paris.

[6] *ANSYS CFX-Solver Theory Guide*, ANSYS, Inc., Southpointe 275 Technology Drive Canonsburg, PA 15317.

[7] Menter F.R., M. Kuntz, R. Langtry. 2003. Ten years of industrial experience with the SST turbulence model. In *Turbulence, Heat and Mass Transfer 4*, (ed.: K. Hanjalic, Y. Nagano and M. Tummers), 625-632. Begell House, Inc.

[8] Mills A.F., R.D. Irwin. 1995. *Basic Heat and Mass Transfer*, University of California, Los Angeles.